Journal of Physics B: Atomic,
Molecular and Optical Physics

PAPER • OPEN ACCESS

Fragmentation and charge transfer in cyclic dipeptides with an aromatic side chain induced by VUV radiation

To cite this article: Laura Carlini *et al* 2024 *J. Phys. B: At. Mol. Opt. Phys.* **57** 105401

View the article online for updates and enhancements.

You may also like

- An Ar valence-shell study by asymmetric (e, 2e) experiments
L Avaldi, R Camilloni, E Fainelli et al.
- Evidence of recent causal decoupling between solar radiation and global temperature
Antonello Pasini, Umberto Triacca and Alessandro Attanasio
- A study of the partial photoionization cross sections of the N_2 valence-shell states
P Bolognesi, G Alberti, D B Thompson et al.

This content was downloaded from IP address 131.175.28.29 on 29/04/2024 at 13:16

OPEN ACCESS
IOP Publishing
Journal of Physics B: Atomic, Molecular and Optical Physics
J. Phys. B: At. Mol. Opt. Phys. **57** (2024) 105401 (15pp)
https://doi.org/10.1088/1361-6455/ad3c00

Fragmentation and charge transfer in cyclic dipeptides with an aromatic side chain induced by VUV radiation

Laura Carlini[1,*], Anna Rita Casavola[1], Jacopo Chiarinelli[1], Francesco Porcelli[1], Elena Molteni[1,2], Giuseppe Mattioli[1], Paola Bolognesi[1], Davide Sangalli[1,2], Federico Vismarra[3,4], Yingxuan Wu[3,4], Rocio Borrego-Varillas[4], Mauro Nisoli[3,4], Manjot Singh[5], Mohammadhassan Valadan[5], Carlo Altucci[5,6,7], Robert Richter[8] and Lorenzo Avaldi[1]

[1] Istituto di Struttura della Materia-CNR (ISM-CNR), Area della Ricerca di Roma 1, Via Salaria km 29.300, 00015 Monterotondo, Italy
[2] Dipartimento di Fisica, Università degli Studi di Milano, Via Celoria 16, I-20133 Milano, Italy
[3] Dipartimento di Fisica, Politecnico di Milano, Piazza Leonardo da Vinci 32, Milano, Italy
[4] CNR-Istituto di Fotonica e Nanotecnologie, Piazza Leonardo da Vinci 32, Milano, Italy
[5] Dipartimento di Scienze Biomediche Avanzate, Università degli Studi di Napoli Federico II, Via Pansini 5, I-80131 Napoli, Italy
[6] Istituto Nazionale Fisica Nucleare (INFN), Sezione di Napoli, Napoli, Italy
[7] Istituto Scienze Applicate e Sistemi Intelligenti-CNR (ISASI-CNR), Via Pietro Castellino 111, 80131 Napoli, Italy
[8] Sincrotrone Trieste, Area Science Park, Basovizza, Trieste, Italy

E-mail: laura.carlini@ism.cnr.it

Received 6 October 2023, revised 25 March 2024
Accepted for publication 8 April 2024
Published 24 April 2024

Abstract

The fragmentation of three cyclic dipeptides (c-Glycil-Phenylalanine, c-Tryptophan-Tyrosine and c-Tryptophan-Tryptophan), characterized by an aromatic side chain, has been investigated by synchrotron radiation and photoelectron-photoion coincidence (PEPICO) experiments, assisted by atomistic simulations. The PEPICO experiments show that the charged moiety containing the aromatic side chain is the main fragment in the three samples. The theoretical exploration of the potential energy surfaces has allowed to identify the possible fragmentation paths leading to the formation of these fragments. Then, the analysis of the differences in the electronic density distributions of the neutral molecule and the cation and a molecular dynamics simulation provided an understanding of the preferred localization of the positive charge on the aromatic side chain of the cyclic dipeptide.

Supplementary material for this article is available online

Keywords: cyclo dipeptides, gas-phase, photoionization and photofragmentation studies, charge transfer processes, molecular dynamics

* Author to whom any correspondence should be addressed.

Original content from this work may be used under the terms of the Creative Commons Attribution 4.0 licence. Any further distribution of this work must maintain attribution to the author(s) and the title of the work, journal citation and DOI.

© 2024 The Author(s). Published by IOP Publishing Ltd

1. Introduction

The role that amino acids and peptides may have played in the appearance of life in the early universe [1], the one that they play in the dynamics of proteins [2] as well as in the development of innovative preparation methods of nanomaterials [3–5], make these compounds an object of widespread interest since the fifties of the previous century.

Peptides are molecules built by a series of amino acids linked via peptide bonds between the carboxyl and amino groups of two adjacent units with the release of a water molecule. Individual peptides are distinguished by the number and sequence of the amino acid residues they contain. A dipeptide is the simplest peptide, obtained by combining two amino acids. Since the first experiments and theoretical simulations [6–10] on the elementary processes occurring in peptides following ionization, the oligo peptide cations (where one of the components is an aromatic amino acid) have been considered the most suited samples to investigate charge transfer and charge migration using the properties of aromatic rings as chromophores. Charge transfer is a dynamic process involving the nuclear degree of freedom, while charge migration is a pure electronic process occurring on femto/attosecond time scale, driven by the electronic coherence of a superposition state or by electron correlations [11, 12] whose experimental investigation has become possible by the advent of ultrafast lasers [13] and Free electron lasers [14]. Charge transfer and charge migration are of considerable interest in physics and chemistry because they allow to couple ionization and chemical reactivity. Moreover, they are of upmost relevance in life science where charge transfer affects the function of proteins [7, 15–17].

Cyclo (c-)dipeptides are dipeptides where the two amino acids are bonded via two peptide bonds with the loss of two water molecules. The simplest of these cyclo-peptides is represented by the cyclo-Glycyl-Glycine (2,5-Diketopiperazine), a six-element ring with three pairs of carbonil, amino and methylene moieties. The other c-dipeptides share the central structure of the 2,5-Diketopiperazine with side chains determined by the residues of the two component amino acids.

In the fifties of the previous century, Stevenson [18] derived from experimental observations an empirical rule stating that in the fragmentation process of a cation the positive charge preferentially resides on the fragment with the lowest ionization potential (IP). Chattoraj *et al* [19] in a pump-probe experiment with a selection of the ionization site on molecules of the type D-Sp-A (where D was a charge donor, A a charge acceptor and Sp a rigid, non-conjugate spacer) observed that the positive charge hops to the chromophore having the lowest ionization energy. Then, Weinkauf *et al* [6] in their studies of linear oligopeptides proved that 'a strong steering of the fragmentation can be engineered' by substitution of various amino acids with different IPs. Similar studies on c-dipeptides do not exist, to our best knowledge.

In this work we have investigated the state selected fragmentation after valence photoionization by synchrotron radiation of three cyclic dipeptides: cyclo Glycil-Phenylalanine ((3S)-3-Benzyl-2,5-piperazinedione), abbreviated as c-GlyPhe in the following, cyclo Tryptophan-Tryptophan ((3S,6S)-3,6-Bis(1H-indol-3-ylmethyl)-2,5-piperazinedione), abbreviated as c-TrpTrp, and cyclo Triptophan-Tyrosine ((3S,6S)-3-(4-Hydroxybenzyl)-6-(1H-indol-3-ylmethyl)-2,5-piperazinedione), abbreviated as c-TrpTyr. These dipeptides share the common feature that at least one of the constituents is an aromatic amino acid. Their side chains contain the phenyl chromophore in c-GlyPhe, the phenol and indole ones in c-TrpTyr and two indole groups in c-TrpTrp.

Here we performed photoelectron-photoion coincidence (PEPICO) spectroscopy, which allows to selectively extract electrons from the occupied orbitals of the neutral system, and therefore, to form cations with different internal energy. Then, the mass spectra measured in coincidence with that photoelectron pinpoint the final localization of the charge. This can provide valuable information on the intramolecular hopping of the positive charge to minimize its energy. The experimental results have been interpreted by means of theoretical exploration of the potential energy surfaces and molecular dynamics simulations. The paper is organized as follows. Sections 2 and 3 are devoted to a brief description of the experimental set-up and procedures and of the theoretical approaches, respectively. The experimental results are described in section 4 and in section 5 they are discussed using the calculated potential energy surfaces, the changes in the electronic density distributions between the neutral molecules and the cations and the molecular dynamics simulations. In section 6 some conclusions are drawn.

2. Experimental methods

The experiments have been performed at the CIPO beamline [20] of Elettra synchrotron facility. The photoelectrons and the photoions have been detected by an electron energy analyzer (VG 220i) and a time-of-flight (TOF) spectrometer, respectively. The two spectrometers are mounted opposite to each other at the magic angle with respect to the polarization vector of the radiation [21]. These two spectrometers can be operated independently, to measure photoelectron spectra and mass spectra, or in conjunction, to perform PEPICO measurements. In the latter kind of experiment, the detection of the kinetic energy resolved photoelectron triggers the extraction of the ions to measure mass spectra correlated to the ionized orbital or, in other words, to the energy deposited in the target molecule by the photoionization process. Recently, the hemispherical analyzer has been equipped with a position-sensitive detector [22, 23] that replaced the original detection system made of six independent channeltrons [21], leading to a significant improvement in terms of efficiency and resolution. A detailed description of the experimental set-up as well as of the experimental procedures can be found in [24].

Both photoemission and PEPICO experiments have been performed at 60 eV photon energy. The PEPICO measurements covered the binding energy (BE) range from the ionization threshold region up to 28 eV. In these experiments the yield of each fragment versus BE is measured. The flight

time of the parent ion from the interaction region to the drift tube entrance of the TOF spectrometer can be estimated as a function of the molecular mass of the molecule, the applied voltages in the extraction/acceleration region and the geometry of the apparatus. In the present work this value is in the range between 1000 and 1500 ns, posing an upper limit to the time of fragmentation to which the experiment is sensitive. The yield of each mass-over-charge, m/z, fragment has been evaluated by integrating the TOF region in the PEPICO spectrum corresponding to a m/z window of approximately ± 0.5 Da. Then, the ratio between the yield of a single fragment with respect to the sum of all observed fragments provides the branching ratio (BR) break-down curve. The first onset of the main fragments has been extracted from a linear fit of their respective yields. Due to the large energy steps in the PEPICO measurements (approximately 200 meV in the present case) and the low statistics close to the onset, the uncertainty of the obtained values (see table 2) of the first onset is rather large. The appearance energy (AE) of a fragment is usually determined by the photoionization efficiency (PIE) measurements, i.e. measuring the ion yield versus photon incident energy. Resonant/autoionizing states which contribute to 'conventional' AE measurements where the photon energy is scanned, cannot be excited in the PEPICO experiments at fixed photon energy and this can alter the value of the measured onset compared to the AE. Moreover, in the case of samples produced by thermal evaporation, the thermal excitation of the molecules may lead to observe a lower appearance threshold. All these aspects have to be considered when comparing the PEPICO onset and the AE obtained in PIE measurements or calculated theoretically, as done in table 2.

The dipeptides are all available commercially, c-GlyPhe (CAS = 10125-07-2, m = 204 Da, purity >98%, Merck Life Science S.r.l.), c-TrpTrp (CAS = 20829-55-4, m = 372 Da, purity >98%, Bachem AG) and c-TrpTyr (CAS = 20829-53-2, m = 349 Da, purity >99%, Bachem AG) and have been used without further purification. Being in the form of powder, they were inserted in a crucible under vacuum and heated at 95, 147 and 155 °C, respectively, to produce an effusive beam. At these temperatures no degradation of the samples occurs. This has been established according to the procedure presented in [25], which involves the measurement of the optical spectra of the pristine sample and of the sample left in the crucible after heating. An example of the procedure is reported in the supplementary information (SI). The residual pressure in the chamber during the experiments was about 5×10^{-8} mbar, while the base pressure was 1×10^{-8} mbar. Typical acquisition times for the PEPICO experiments were in the range of 16–20 h for each sample.

Preliminary tests of the evaporation of the samples with a TOF mass spectrometer and a He lamp [26] have shown that the samples contain traces of precursors used in the synthesis. This has been identified observing an anomalous behavior of the intensity of some fragments with respect to the one of the parent ion versus temperature. In particular, this has been observed for fragments at m/z 130 in c-TrpTrp and 130 and 107 in c-TrpTyr.

3. Theoretical details

The AE is defined as the minimum energy that must be supplied to a gas-phase molecule in order to produce a particular fragment ion. Theoretically, the AE is calculated as the difference between the energy of the ground state of a fragment and that of the neutral parent molecule, i.e. the adiabatic energy of the fragmentation process. Quantum chemistry calculations have been performed at the level of density functional theory (DFT). The geometries were optimized using the three-parameter Becke Lee-Yang-Parr (B3LYP) functional with the 6–31G basis set. Accurate total energies were obtained by single-point coupled cluster calculations (CCSD) [27] using the same basis sets for the B3LYP calculations. All calculated energies include the zero point energy correction calculated at the DFT level of theory. All calculations were performed using Gaussian 09 [28]. In the calculations of the AE a temperature of 298.15 K has been assumed.

The height of the barrier, i.e. the energy of the transition state (TS), is clearly not taken into account in the adiabatic calculation and has to be estimated separately when the observed AE is greater than the theoretical one. In these cases we have used a synchronous transit-guided quasi-newton method, at the B3LYP/6-31 G level of theory [29] in order to obtain the TS between selected initial and final configurations. The TS were unambiguously related to their interconnected energy minima by intrinsic reaction coordinates calculations [30, 31]. Accurate total energies for the TSs were obtained by CCSD calculations [27] using the same basis sets for the B3LYP calculations. The energy barrier is then calculated as the energy difference between the initial and intermediate states.

In [32] we have reported an accurate theoretical investigation of the energetics of the three molecules under investigation by comparing dispersion corrected tight-binding, dispersion corrected DFT and CCSD(T) calculations. Then, different first principles computational schemes have been considered to simulate the photoemission spectra. In detail, we have compared cost-effective approaches based on direct use of Hartree–Fock and Kohn–Sham (e.g. B3LYP) orbitals with accurate, state-of-the art methods involving perturbative quasi-particle GW corrections of Kohn–Sham orbitals or the calculation of ionization energies at the EOM-CCSD level of theory. Such comparison indicated that DFT B3LYP calculations provide a reasonably good description of both the energy distribution of occupied electronic states (after application of an appropriate rigid shift to all B3LYP occupied levels in order to match the experimental ionization energy) and the spatial localization of the corresponding electronic charge involved in the ionization process, in agreement with EOM-CCSD results but at a fraction of its computational cost.

In view of the above-mentioned considerations on the validation of DFT B3LYP calculations versus EOM-CCSD ones and experimental photoelectron spectra, we have performed electronic structure calculations for the cationic forms of the three investigated cyclo-dipeptides within plane-wave DFT B3LYP using the Quantum ESPRESSO package [33, 34], with the same overall computational details as in [32], in

order to compare the spatial localization of frontier orbitals of the three molecular cations with that of the corresponding neutral molecules. For molecular cations, we performed spin-polarized collinear calculations, setting the total charge to +1 and the multiplicity to 2; density difference distributions shown and discussed below have been obtained by subtracting from the total electronic density of the neutral molecules the total electronic density of the molecular cations, kept fixed in the optimized geometry of the former ones. Experimental mass spectra have been calculated using the QCxMS code [35, 36], and a detailed description of the computational protocol is provided in the SI.

4. Results

The structure of the three cyclic dipeptides consists of a central diketopiperazine (DKP) ring and different side chains depending on the constituent amino acids, which contain the phenyl, phenol and indole chromophore groups in Phe, Tyr and Trp amino acids, respectively (figure 1). Due to the flexible structure of their –CH_2–R side chains, these molecules exist in different rotameric conformations. The free energies of the most populated conformers differ only by a few mHa [32], thus the contribution of the different conformers to the photoelectron spectra cannot be resolved.

The photoelectron spectra of the three molecules and their simulations using different first principles computational schemes have been recently published [32]. Here the spectra (figure 2) will be only briefly described in order to be used as a guide for the interpretation of the PEPICO spectra. The three photoelectron spectra share some common features, namely a first feature in the 7–11 eV BE region, followed after a gap by broader features which display a maximum intensity around 14 eV. In the first region two structures are clearly visible in the spectra of c-TrpTrp and c-TrpTyr, which merge in a single feature in the c-GlyPhe case.

Despite some discrepancies in the absolute value reported in the literature, the experimental IP of the aromatic amino acids [37–41] increases going from Trp to Tyr and Phe. The energy of the first feature in the experimental photoelectron spectra [32] in figure 2 increases from 7.97 ± 0.04 eV in c-TrpTrp, to 8.18 ± 0.04 eV in c-TrpTyr and 9.54 ± 0.02 eV in c-GlyPhe, following the same trend of the constituent aromatic amino acids. These values and the analysis of both electronic densities of states and spatial localization of molecular orbitals, done in [32] and partially reported in the SI, confirm the role of the side chain of the aromatic amino acid in determining the energy of the outermost orbitals and therefore the chemical-physical properties of these cyclo-dipeptides. The close values of the IP of Phe and Gly [37, 42, 43] explain also the merging of the two peaks in a single feature in c-GlyPhe. These findings are consistent with previous observations in the photoelectron spectra of other c-dipeptides containing amino acids with an aromatic side chain [44, 45]. As pointed out in [32], the IPs of the cyclic dipeptides, higher than those of the constituent aromatic amino acids, are a sign of the stability (screening) effect primarily induced by electron-rich C=O groups of the DKP ring on the chromophores of the side chain.

Figures 3(a)–(c) show the mass spectra of the three samples, obtained by adding up all the PEPICO spectra measured in the BE region up to 28 eV for c-GlyPhe and up to 24 eV for c-TrpTrp and c-TrpTyr. In the case of c-TrpTrp and c-TrpTyr an expanded view of the region m/z 200–260 is shown in an inset. The m/z of the main fragments is indicated in the figures and their proposed assignments [46–48] are reported in table 1. The parent ion gives a significant contribution to the c-GlyPhe spectrum, while it is barely observed in the spectra of the other two samples. In all cases the fragment with the aromatic residue (phenyl in c-GlyPhe and indole in c-TrpTrp and c-TrpTyr), having the lowest ionization energy, dominates the spectrum. Only in the case of c-GlyPhe the complementary moiety (m/z 113) is observed with some intensity, while in the other two cases, the fragments at m/z 242 and 219 for c-TrpTrp and c-TrpTyr, respectively, (see the insets in figures 2(b) and (c)) show a negligible intensity, below 1% with respect to the intensity of the fragment at m/z 130. It is also interesting to note that the fragment assigned to the phenol residue (m/z 107) in c-TrpTyr gives a very small contribution to the spectrum.

Even though the contribution of double ionization cannot be completely excluded in the BE >20 eV, the spectrum is expected to be dominated by single ionization events and no clear evidence of doubly charged ions has been detected.

4.1. PEPICO measurements of c-GlyPhe molecule

The structure of this dipeptide (figure 1) is made by a central DKP ring and a phenyl side chain connected through a flexible –CH_2– bridge. The main features of the sum of all PEPICO spectra in figure 3(a) have been assigned in table 1 according to the previous literature [25, 46–48]. The parent cation is clearly visible at m/z 204; the C_7H_7 ion (m/z 91) and its complementary fragment $[C_4H_5N_2O_2]^+$ (m/z 113) may be attributed to the benzyl residual or its loss from the parent ion; the $[C_3H_5N_2O]^+$ (m/z 85) may result from a further CO loss from m/z 113 with two bond breaks and the opening of the ring; the feature at m/z 65 has been assigned to the loss of acetylene C_2H_2 from the $C_7H_7{}^+$ producing the C_5H_5 ion; fragments at m/z 43 and 30 may be tentatively assigned to further fragmentations of $C_3H_5N_2O$ and $C_4H_5N_2O_2$ cations.

The results of the PEPICO experiments, i.e. the state-selected fragmentation of c-GlyPhe molecule, are summarized in figure 4. In figure 4(a) the PEPICO relative ion yields as well as the photoelectron spectrum (bottom panel) are reported. This representation allows to investigate possible correlations among the ionized orbital, or the energy transferred to the neutral molecule, and the yield of the different fragments. In figure 4(b) the BRs for each fragment are shown. This is an alternative representation of the same data reported in figure 4(a) and provides more direct information on the relevance of each channel, a better definition of their onset and may allow to establish correlations among the fragmentation pathways.

In both figures only fragments which contribute more than 4% to the BR are shown. Due to this choice, the fragment at

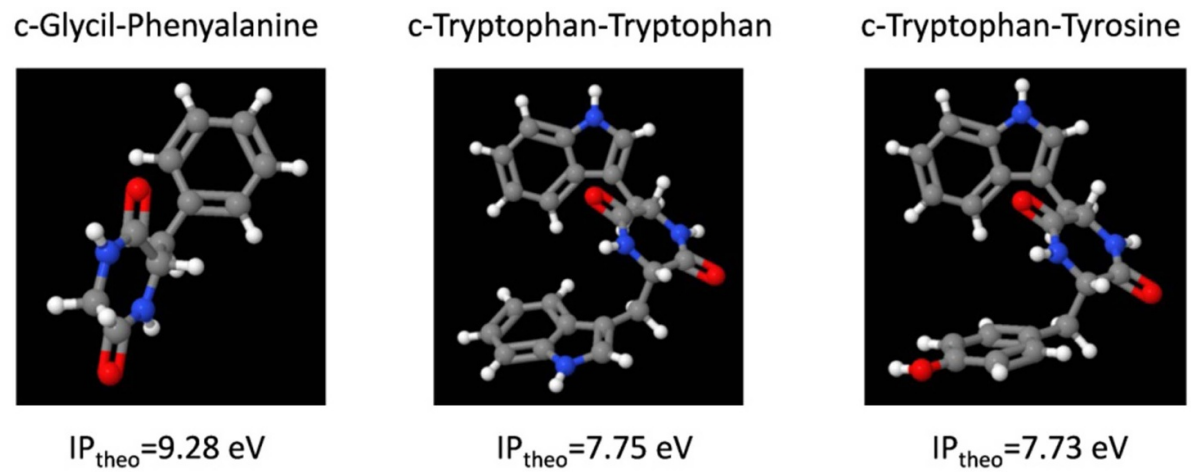

Figure 1. The structure of c-GlyPhe, c-TrpTyr and c-TrpTrp and the vertical theoretical ionization energies calculated at the EOM-CCSD level of theory from [32].

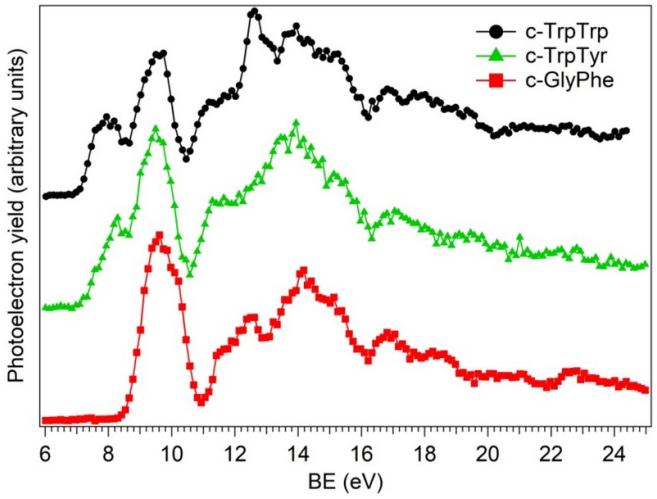

Figure 2. Comparison between the photoemission spectra of c-TrpTrp (black curve), c-TrpTyr (green curve) and c-GlyPhe (red curve) measured at 60 eV photon energy. The maximum of the first feature is at 7.97 ± 0.04, 8.18 ± 0.04 and 9.54 ± 0.02 eV in c-TrpTrp, c-TrpTyr and in c-GlyPhe, respectively. The feature at 12.6 eV in the c-TrpTrp photoelectron spectrum is due to residual water in the sample.

m/z 43, that in the sum of all PEPICO spectra (figure 3(a)) is clearly observed with an intensity higher than, for example, the m/z 65 one, but never reaches a BR of 4% at any BE, has not been reported in figure 4. The overall contribution of all minor fragments has been arbitrarily organized in two groups, according to their common trend versus BE: the sum of m/z 15, 42, 39, 51, 56, 77 and 78, named SUM1, includes the minor contributions of fragmentation channels opening above 16 eV. Fragments with m/z 43, 57, 58, 103, 104, 118, 119, 120 and 131, which correspond to fragmentation channels opening at about 11 eV and observed up to 25 eV, have been added in SUM2.

The parent ion, m/z 204, is observed in the region from the IP up to about 11.6 eV. According to the DFT calculations of [32], the outermost valence molecular orbitals from the HOMO to the HOMO-9 are located in this region. The 113^+ and 91^+ fragments, resulting from the break-up of the cyclo-dipeptide in two complementary moieties, correspond to the diketopiperazine central ring (mass 113 Da) and the benzyl group (mass 91 Da). They practically appear at about the same energy (around 9.7 eV), but show a completely different BR. The 113 ion gives a minor contribution with a BR $\leqslant$ 10% and it is observed only up to 12 eV; vice versa the 91 ion is the dominant fragment. From the onset, its relative intensity grows to a first relative maximum at 10.3 eV and then follows the shape of the photoelectron spectrum. Its BR varies from about 86% at BE = 10.8 eV down to 34% at 19 eV, then remains around 30% up to 29 eV. This shows that, independently of the energy left in the molecule and the ionized orbital, the preferential break-up channel leads to the formation of the 91^+ fragment which is quite stable. The 85^+ fragment, with PEPICO onset at 10.4 ± 0.8 eV, is observed in a well-defined BE range centered around 15 eV. The fragmentation channels leading to 65^+, 30^+ and 28^+ fragments open above BE = 14 eV, but while the relative yield and BR of m/z 30 increase from its AE up to 16.9 eV and then decrease, in the case of the other two fragments, 65^+ and 28^+, their BR increases with the BE.

4.2. PEPICO measurements of c-TrpTrp and c-TrpTyr molecules

The structure of these dipeptides, shown in figure 1, is characterized by the same central DKP ring with two side chains containing two indole groups in the case of c-TrpTrp and one indole and one phenol group in the case of c-TrpTyr. The main features observed in the sum of all PEPICO spectra and their proposed assignments are reported in table 1. As shown in figure 3, the m/z 130 fragment dominates the spectrum, while the parent ion and few smaller fragments show a tiny contribution for both c-TrpTrp and c-TrpTyr. Other than the 130^+ fragment, which can be attributed to the indole–CH_2 chromophore fragment, the two dipeptides display some common fragments (77^+, 85^+, 103^+, 113^+, 114^+, 117^+, 241^+, 242^+ and 243^+)

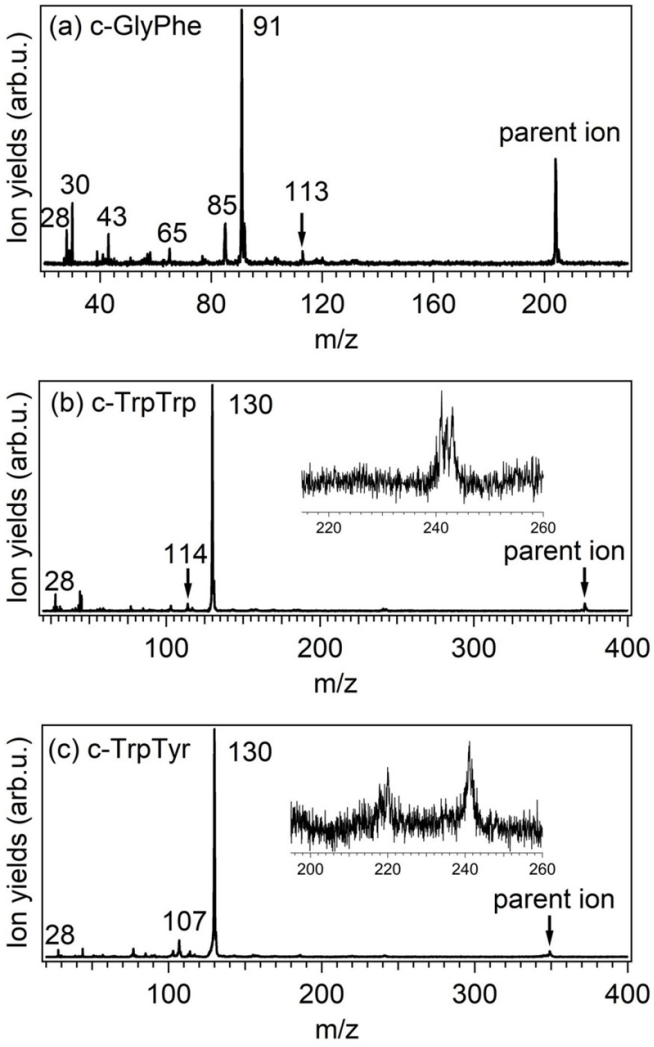

Figure 3. Sum of all PEPICO spectra of c-GlyPhe (a), c-TrpTrp (b) and c-TrpTyr (c) up to BE 28 eV in the case of c-GlyPhe and 24 eV in the other two cases, acquired at 60 eV photon energy. Some of the main fragments are indicated and the proposed assignments are reported in table 1. The insets show an expanded view of the m/z region 220–260 and 200–260 for c-TrpTrp and c-TrpTyr, respectively.

likely related to similar fragmentation pathways. The parent cations are barely observed at m/z 372 and m/z 349 for c-TrpTrp and c-TrpTyr, respectively. Fragment $[C_9H_8N]^+$ at m/z 130, corresponding to the fragment with the indole side chain, dominates completely the spectra, while the complementary fragments at m/z 242 for c-TrpTrp and m/z 219 for c-TrpTyr (see the insets in figures 3(b) and (c)) show an intensity ratio $<1\%$ with respect to the 130 ion. The m/z 85 may be assigned to $[C_3H_5N_2O]^+$ produced in a fragmentation pathway similar to the one observed for c-GlyPhe, in this case with the loss of CO and COH from fragments $[C_4H_5N_2O_2]^+$ (m/z 113) and $[C_4H_6N_2O_2]^+$ (m/z 114), respectively. The features at m/z 117, 103 and 77 have been assigned to the subsequent fragmentation of the $[C_9H_8N]$ cation with the loss of CH, CH_2 and C_2H_2, respectively; the fragment at m/z 107 in the c-TrpTyr

Table 1. Proposed assignment of the main features in the mass spectra of c-GlyPhe, c-TrpTrp and c-TrpTyr shown in figure 3. 'x' indicates the presence of the fragment in the mass spectrum of the molecule.

m/z	c-GlyPhe	c-TrpTrp	c-TrpTyr	Proposed assignments
28	x	x	x	CO^+
30	x			CH_2O^+; $CH_2NH_2^+$
43	x			$HNCO^+$; $C_2H_5N^+$
44		x	x	CH_2NO^+; $C_2H_6N^+$
65	x			$C_5H_5^+$
77	x	x	x	$C_6H_5^+$
85	x	x	x	$C_3H_5N_2O^+$
91	x			$C_7H_7^+$
103		x	x	$C_8H_7^+$
107			x	$C_7H_7O^+$
113	x		x	$C_4H_5N_2O_2^+$
114		x	x	$C_4H_6N_2O_2^+$
117		x	x	$C_8H_7N^+$
130		x	x	$C_9H_8N^+$
204	x			c-GlyPhe parent cation
241		x	x	$C_{13}H_{11}N_3O_2^+$
242		x	x	$C_{13}H_{12}N_3O_2^+$
243		x	x	$C_{13}H_{13}N_3O_2^+$
349			x	c-TrpTyr parent cation
372		x		c-TrpTrp parent cation

mass spectrum can be assigned to the other aromatic terminal, the phenol-CH_2 terminal of the Tyr amino acid ($[C_7H_7O]^+$).

The PEPICO relative yields of the fragments which contribute with more than 4% to the BR are reported for c-TrpTrp and c-TrpTyr in the left and right panels of figure 5, respectively. Given the large predominance of only the fragment 130^+, no BRs have been reported in a separate figure. The parent ion is detected in the BE region between 6.5 and 10 eV for both molecules. The fragmentation channel leading to the 130 cation ($[C_9H_8N]^+$) opens at very low BE (around 8 eV, as reported in table 2), and fully reproduces the shape of the photoelectron spectrum. Fragments 241–242-243 and 113–114 have been grouped together as they cannot be fully resolved in the PEPICO mass spectra.

The only other fragment with a reasonable contribution to the PEPICO yield is the 107 cation ($[C_7H_7O]^+$), which corresponds to the Tyrosine aromatic terminal of c-TrpTyr molecule (figure 5, right side).

In figure 5, an appreciable PEPICO yield of 130^+ fragment in the case c-TrpTrp and 130^+ and 107^+ in c-TrpTyr has been observed also below the reported PEPICO onset in table 2 and very close to the onset of the parent ion. This signal has been attributed to impurities, likely precursors in the synthesis that have an IP lower than that of the c-dipeptide. This explanation is supported by preliminary tests of thermal desorption of the samples, where the relative intensities of these fragments with respect to the parent ion has been monitored over time, showing a decreasing trend with time/temperature, up to a stable ratio (see figure S1 in the SI). This suggests that these ions could have two possible sources: a pollutant present in trace that decreases with time/temperature and

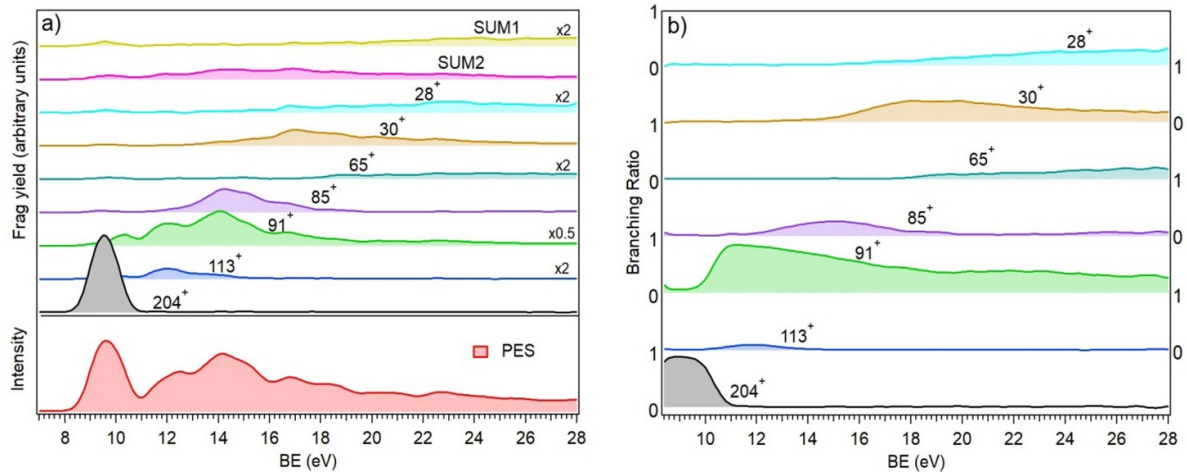

Figure 4. Left panel: bottom panel—the photoelectron spectrum of the c-GlyPhe molecule measured at 60 eV photon energy; top panel—PEPICO yields of the main fragments. All minor fragments have been added into SUM1 and SUM2 (see text). Right panel: branching ratios (BRs) of the fragment ions. Only fragments whose contribution is higher than 4% of the total intensity at each given BE are reported.

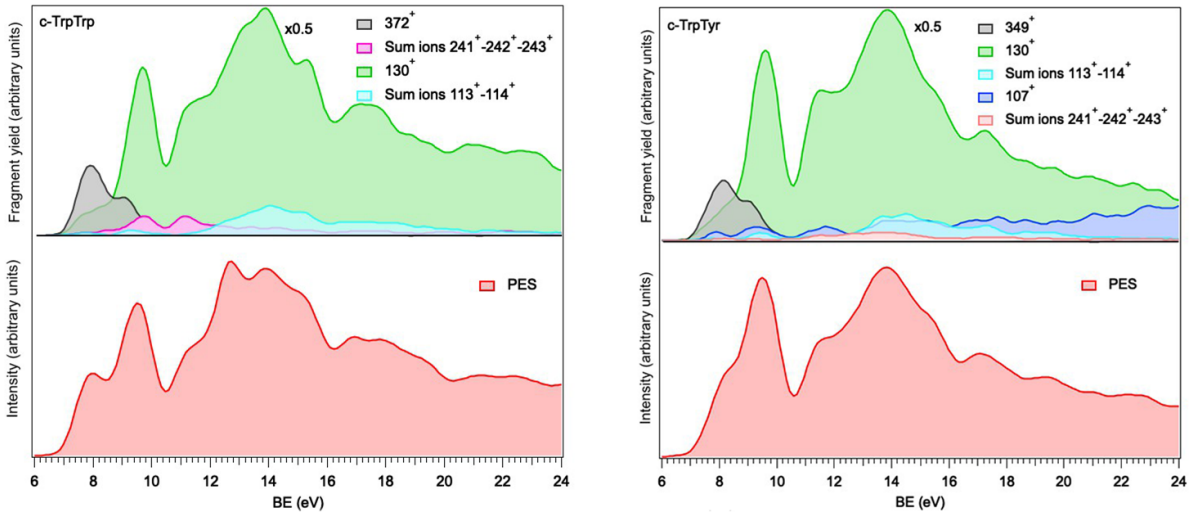

Figure 5. PEPICO yields of the main charged fragments showing contributions with BR $>$ 4% of the total intensity compared with the PES (red curve) for c-TrpTrp (left panel) and c-TrpTyr (right panel).

a fragment produced by molecular fragmentation, with stable relative intensity compared to parent ion.

5. Discussion

Quantum chemistry calculations have been performed to identify the most relevant fragmentation channels observed in the PEPICO experiments and the structure of the produced compounds. In figure 6 it is shown that after ionization c-GlyPhe may break in the two moieties of masses 113 and 91 Da, with potential energy barriers that almost coincide with the formation energy of the two fragments. The formation of C_7H_7 cation is slightly favored from an energetic point of view with respect to the formation of m/z 113. The predicted difference between the two theoretical onsets (0.2 eV) is comparable with the experimental uncertainty (table 2), thus the onset of the two channels could not be distinguished in the experiment. The dominance of the 91^+ fragment over the 113^+ can be explained by the instability of the latter that undergoes further fragmentation at about 10 eV BE. This is clearly demonstrated in the potential energy surfaces (figure 6) that show how 113^+ can break in a charged five element ring of mass 85 Da and CO. The 85^+ fragment can be formed in two isomeric structures that can be reached via a single TS at 11.47 eV or in two steps with a TS at 10.87 eV. The latter is the energetically favored one. The experimental PEPICO onset of 85^+ is consistent with the calculated value. The alternative paths, leading to the two neutral isomers with mass 85 Da and CO^+, have been also evaluated with an AE above 17 eV.

The reaction pathway, molecular structures and energy barriers leading to the production of 65 ion from 91^+ after the loss of C_2H_2 (mass 26 Da) have been also studied, while the ones leading to the production of 30^+ have not been investigated

Table 2. The main fragmentation channels observed in the PEPICO measurement, the proposed assignments of the different fragments, the calculated AE of the fragments and the first onsets estimated from the PEPICO relative yields and BRs. The large uncertainty (>0.5 eV) for the onset of some fragments is related to the low signal to noise ratio in a region of vanishing signal. We do not report the AE of fragment 241^+, as several paths may lead to the formation of this ion hampering the calculation of its energy and the investigation of this fragment is not particularly relevant in the framework of this study.

Molecule	Fragment	Assignment	Theoretical AE [eV] (adiabatic IP)	PEPICO onset [eV]
c-GlyPhe	204^+	parent cation	8.49	7.9 ± 0.2
	113^+	$C_4H_5N_2O_2^+$	9.93	9.7 ± 0.3
	91^+	$C_7H_7^+$	9.67	9.7 ± 0.2
	$85^+(1)$	$C_3H_5N_2O^+$	10.76 (TS1) → 10.87 (TS2) → 10.01	10.4 ± 0.8
	$85^+(2)$		11.47 (TS) → 9.15	
	65^+	$C_5H_5^+$	12.45 (TS)→ 16.07	17 ± 0.5
c-TrpTrp	372^+	parent cation	6.83	7.1 ± 0.4
			8.08 (direct dissociation from parent ion)	
	130^+	$C_9H_8N^+$	10.54 (from 242^+ after the loss of 112)	8.5 ± 0.4
			12.07 (from 243^+ after the loss of 113)	
	241^+	$C_{13}H_{11}N_3O_2^+$	_____	
	242^+	$C_{13}H_{12}N_3O_2^+$	8.29	8.5 ± 0.3
	243^+	$C_{13}H_{13}N_3O_2^+$	10.81	
	113^+	$C_4H_5N_2O_2^+$	13.66	11.0 ± 0.9
	114^+	$C_4H_6N_2O_2^+$	16.78	
c-TrpTyr	349^+	parent cation	6.18	7.0 ± 0.4
			8.13 (direct dissociation from parent ion)	
	130^+	$C_9H_8N^+$	10.50 (from 242^+ after the loss of 112)	8.2 ± 0.3
			12.44 (from 243^+ after the loss of 113)	
	241^+	$C_{13}H_{11}N_3O_2^+$	_____	
	242^+	$C_{13}H_{12}N_3O_2^+$	8.24	8.5 ± 0.2
	243^+	$C_{13}H_{13}N_3O_2^+$	11.19	
	113^+	$C_4H_5N_2O_2^+$	14.03	11.5 ± 0.7
	114^+	$C_4H_6N_2O_2^+$	17.15	
	107^+	$C_7H_7O^+$	8.90 (direct dissociation from parent ion)	8.1 ± 0.4
			11.36 (from 219^+ after the loss of 112)	

as this fragment may be generated with different molecular structures via different dissociation pathways and following rearrangements of fragments 113^+ and 85^+. From the benzyl fragment (91^+) the $C_5H_5^+$ (m/z 65) ion and the neutral C_2H_2 fragment can be produced. $C_5H_5^+$ is quite unstable and can fragment into $C_3H_3^+$ (m/z 39) and a neutral acetylene molecule. The 39^+ fragment is observed in the sum of all PEPICO spectra (figure 3(a)), but its relative yield in the different PEPICO spectra is always less than 4%.

In the following, the molecular fragmentation channels of c-TrpTrp and c-TrpTyr will be discussed together due to the many similarities between these two molecules. As shown in figures 7(a) and (b), different channels can lead to the production of 130^+ ion for both c-TrpTrp and c-TrpTyr. The one showing the lowest AE corresponds to the direct dissociation of parent ion into 130^++242 (8.08 eV) and 130^++219 (8.13 eV) for c-TrpTrp and c-TrpTyr, respectively. In the case of c-TrpTrp, due to the symmetry of the molecule and supported by the calculated AE (see figure 7(a)), the channel leading to 130^+ and 242 fragments appears to be the favored one. Two other channels for the production of fragment 130^+ have been also investigated. They involve the loss of 112 and 113 from 242^+ and 243^+, with AE's of 10.54 eV and 12.07 eV, respectively.

For the case of c-TrpTyr, three different reaction pathways which start directly from the parent ion have been identified and reported in figure 7(b). Pathway 1 (black line) shows the direct dissociation of the parent ion into two moieties of masses 130 and 219, with the lowest AE for the production of 130^+ (8.13 eV). On the contrary, the phenol-CH_2 fragment (107 Da) in the other side chain of the molecule can be produced after subsequent fragmentation of 219^+ into 107^+ and 112 and shows an AE above 11 eV. The second reaction pathway (green line) shows the formation of 107^+ after the loss of 242 directly from the parent ion with an AE of 8.9 eV, definitely lower than the one obtained in pathway 1, and the formation of 242^+ and neutral 107 with AE = 8.24 eV. Then, as in the case of c-TrpTrp molecule, the 130^+ ion can be produced after the loss of neutral 112 from 242^+ with AE of 10.5 eV. Finally, the direct dissociation of parent ion into 106–243^+ (pathway 3, blue line) can lead once again to the production of 130 ion after the loss of 113 from 243^+ with AE above 12 eV.

The exploration of the potential energy surfaces has allowed to understand the main channels leading to the different fragmentations observed in the PEPICO spectra, however it does not explain the large dominance of the m/z 91 and 130 in c-GlyPhe and c-TrpTrp/c-TrpTyr PEPICO yields, respectively. The main characteristic of the PEPICO experiments is

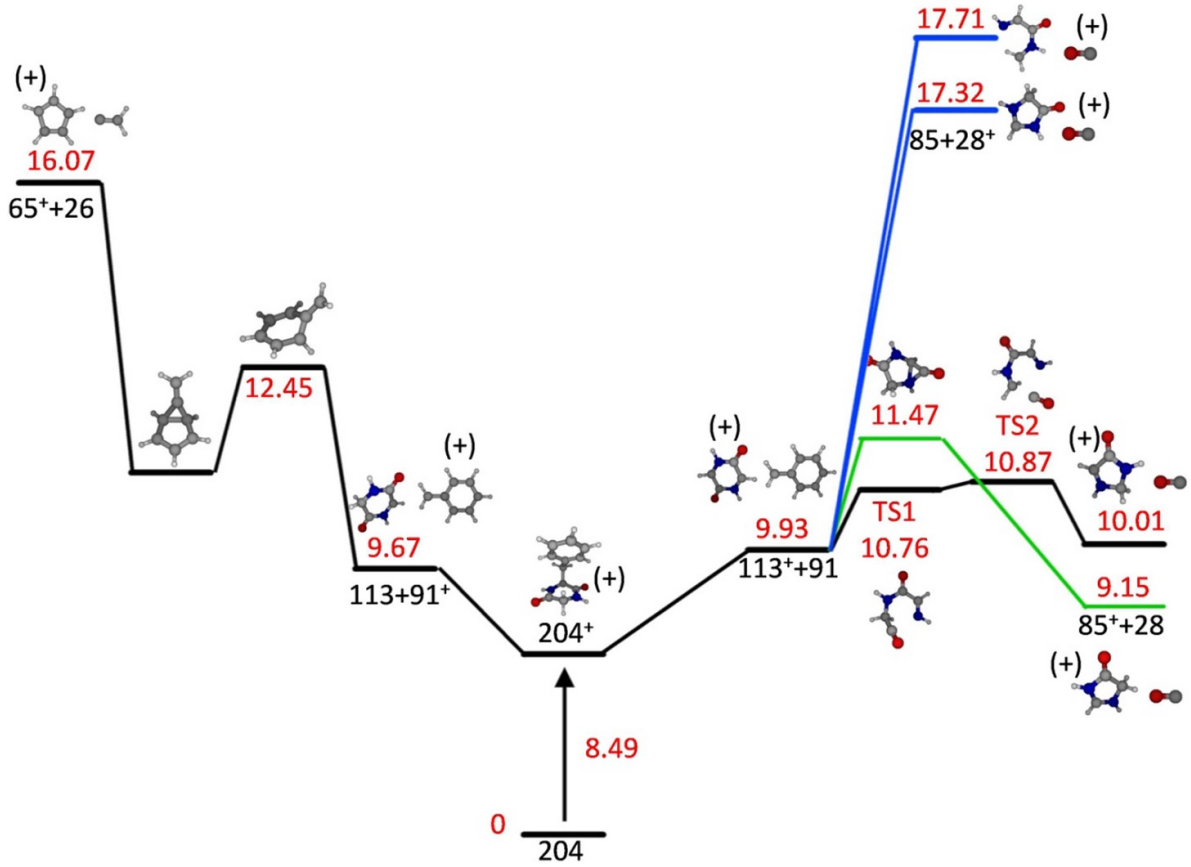

Figure 6. The most probable fragmentation pathways for the c-GlyPhe dipeptide. Molecular structure, fragment energy and m/z are reported.

the capability to correlate a fragmentation mass spectrum to the energy transferred to the target, and therefore, the state or the band of states (depending on the experimental resolution) from which the electron is extracted and the hole is created. The experimental observation that, independently on the energy transferred, certain charged fragments containing the aromatic chromophore are mainly produced is consistent with the idea that the photoionization is followed by an internal conversion to the ground state of the cation with a redistribution of the energy transferred into intramolecular vibrations. Such process is at the base of successful statistical theories of unimolecular reactions [49, 50]. Intramolecular charge hopping after photoionization has been observed in the past [19, 51] in presence of an aromatic terminal such as benzene, indole, and biphenyl, with no intrinsic restriction for the distance of the charge migration. In this process the hole relaxes to the HOMO, to optimize the total energy of the system and then, if the residual vibrational excitation is larger than the barrier to the dissociation, the cation fragments with the charge left on the moiety containing the aromatic chromophore, which is the one with the lowest IP.

This can be visualized considering the electronic densities of states and spatial localization of the molecular orbitals in both the neutral molecule and cation. In [32] an accurate analysis of the electronic densities of states and spatial localization of the molecular orbitals for the neutral molecules c-GlyPhe, c-TrpTrp and c-TrpTyr has been reported. The comparison between the experimental photoelectron spectra of the three molecules and the calculated density of states suggests that typical fingerprints can be assigned to the presence of the DKP ring and of at least one aromatic residual group in all the samples investigated here. In the region 8–10 eV (see figure 2), the IP is determined by π-orbitals of the aromatic rings [32]. A second sub-structure in this energy region is detected for c-TrpTrp and c-TrpTyr, this structure shows contributions also from the orbitals localized on the C=O–NH blocks of the DKP ring. In the case of c-GlyPhe (red spectrum in figure 2), the two structures merge in a single feature as the IP of the phenyl ring is very close to the DKP ring one. Then at higher energies there is a region for all the three molecules with a high density of electronic states lying in the planes of the aromatic rings, mainly due to the sp2 orbitals of carbon atoms. According to DFT calculations of the neutral molecules [32] the charge in the outer valence levels is alternately localized on the Phe and DKP rings in the case of c-GlyPhe, on one of the two residual groups of the Trp amino acid for c-TrpTrp and on the indole and phenol ring in one of the two side chains of c-TrpTyr, as reported in the SI. Similar calculations of the charge distribution of the molecular orbitals have been performed also for the cations. The full results of spin-polarized DFT calculations carried out on the cations for all the three samples here investigated have been reported in the supporting information. Here

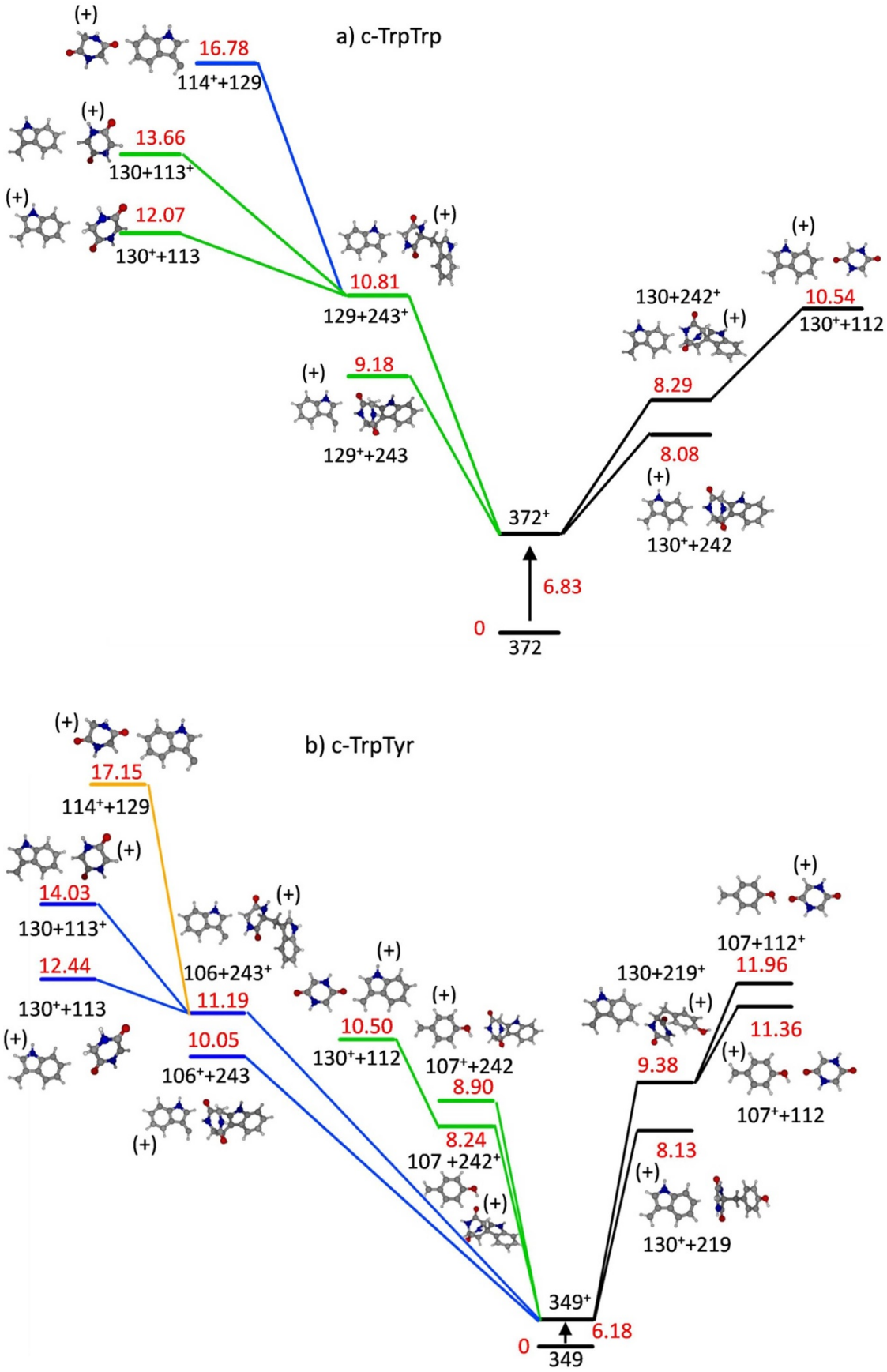

Figure 7. The most likely fragmentation pathways for the c-TrpTrp (top panel) and c-TrpTyr (bottom panel) dipeptides. Molecular structure, fragment energy and m/z are reported. The main fragmentation channels for both molecules are discussed in the text.

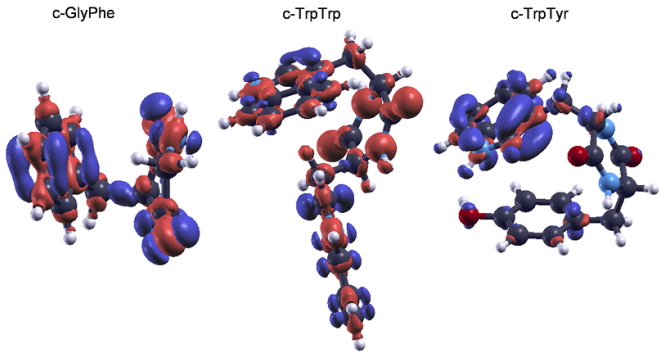

Figure 8. Maps of the difference of the electronic density distribution between the neutral molecules and cations. Red and blue regions indicate positive and negative differences, respectively.

we summarize them using the difference map of the total electronic density distributions, i.e. the electronic density distribution summed over all the valence orbitals, in the cation and neutral molecule to provide a simplified yet sound explanation of the experimental results. The red regions in these maps indicate positive differences, while the blue ones indicate negative differences. Thus, the areas showing more and/or larger blue region correspond to a lower electronic density in the case of cation with respect to the neutral molecule. This graphical analysis provides information on how the charge redistributes after ionization and provides some understanding of the localization of the positive charge in the molecular fragmentation. In figure 8, the difference maps of the total electronic density distributions for the three studied molecules are shown.

In the case of c-GlyPhe (left panel in figure 8), the regions involved in the depletion and accumulation of charge upon ionization are distributed on both Phe and DKP rings. The dominance of the blue depletion region on the phenyl residual group suggests that the positive charge would be preferentially localized on the aromatic ring. Thus, during the fragmentation of the cation the release of the 91^+ fragment is expected to be privileged, in good agreement with the PEPICO results where a propensity towards the release of the phenyl residual group has been observed.

Due to the symmetry of the molecule in case of c-TrpTrp (center panel in figure 8), we observe blue depletion regions almost equally distributed on the two indole rings of the side chains. This confirms that after ionization the positive charge preferentially floats on the Trp side groups, which are eventually lost as charged fragments.

Finally, in the case of c-TrpTyr reported on the right panel of figure 8, the analysis of the difference of the electronic density distribution points out once again that the positive charge preferentially resides on the aromatic group of the Trp amino acid, which has the lowest IP. All these observations are qualitatively consistent with the PEPICO results.

In [32] the spatial localization of the HOMO B3LYP bound electronic states with that of the weighed superposition of the HF states mostly contributing to the EOM-CCSD ionization energies have been compared in the case of c-GlyPhe. As shown in figure 5 of that paper, the analysis of both electronic densities of states and spatial localization of molecular orbitals proves that DFT B3LYP calculations provide a reasonably good description of the electronic properties, if compared to the EOM-CCSD approach, but at a much lower computational cost. This justifies the use of the B3LYP 'molecular orbitals' for the analysis of the difference of the electronic density distribution done here. In the SI a similar analysis has been extended to c-TrpTrp and c-TrpTyr molecules.

A complementary point of view on dynamical effects inducing the fragmentation of the investigated molecules after ionization is provided by tight-binding molecular dynamics simulations. Such simulations have been used to calculate theoretical mass spectra, as detailed in the SI. These calculated spectra, shown in figure S7, display a reasonable agreement with the experimental results, providing solid ground for the dynamical analysis of fragmentation discussed in the following. In all computed spectra, characteristic fragmentations are observed, with the most abundant 91^+ fragment appearing for c-GlyPhe, and 130^+ fragment appearing for c-TrpTrp and c-TrpTyr.

The simulations performed on c-TrpTyr show that ionization induces a fast (10∼15 ps at 300 K) structural rearrangement of the neutral molecule. The stable folded neutral structure, shown in figure 1, is converted after ionization into an 'open structure' with the aromatic groups kept far from each other (see figures 9–11). As detailed below, the localization of the positive charge on the side chains in such structure induces an electrostatic repulsion between the aromatic groups. This electrostatic repulsion is stronger than the attraction based on dispersion forces which, on the contrary, dominates the evolution at finite temperature of the neutral molecules. A more detailed analysis has been then carried out on specific fragmentation processes in order to shed light on the correlation between dynamical evolution of molecular structure and intramolecular charge distribution.

In figure 9 the transition from the parent ion of c-TrpTyr (349^+) to the neutral 242 and charged 107^+ fragments is characterized by a swift charge migration from the indole group to the phenol substituent, as indicated by the extent of charge depletion (blue regions) across the trajectories. More specifically, within an interval of 100–200 fs, the positive charge moves from the indole ring to the DKP and phenol rings, accompanied by an increase in the CH_2–CH distance on the side of the indole group (red arrows). After such a rearrangement of the electronic charge, the 107^+ fragment is ready to detach from the molecule in a further outward oscillation of the CH_2–CH bond on the side of phenol (black arrows). A similar interplay between the oscillation of electronic charge and that of selected bonds is found along different trajectories leading to the formation of different fragments.

The production of fragment 242^+ from the parent ion is depicted in figure 10, where a notable charge depletion on the indole terminal group is accompanied by a CH_2–CH bond oscillation with the final production of 242^+ fragment. It is interesting to note that after the formation of 242 ion, the strict localization of positive charge on the indole substituent within the fragment 242^+ is accompanied by an increase in the CH_2–CH distance between indole and DKP rings

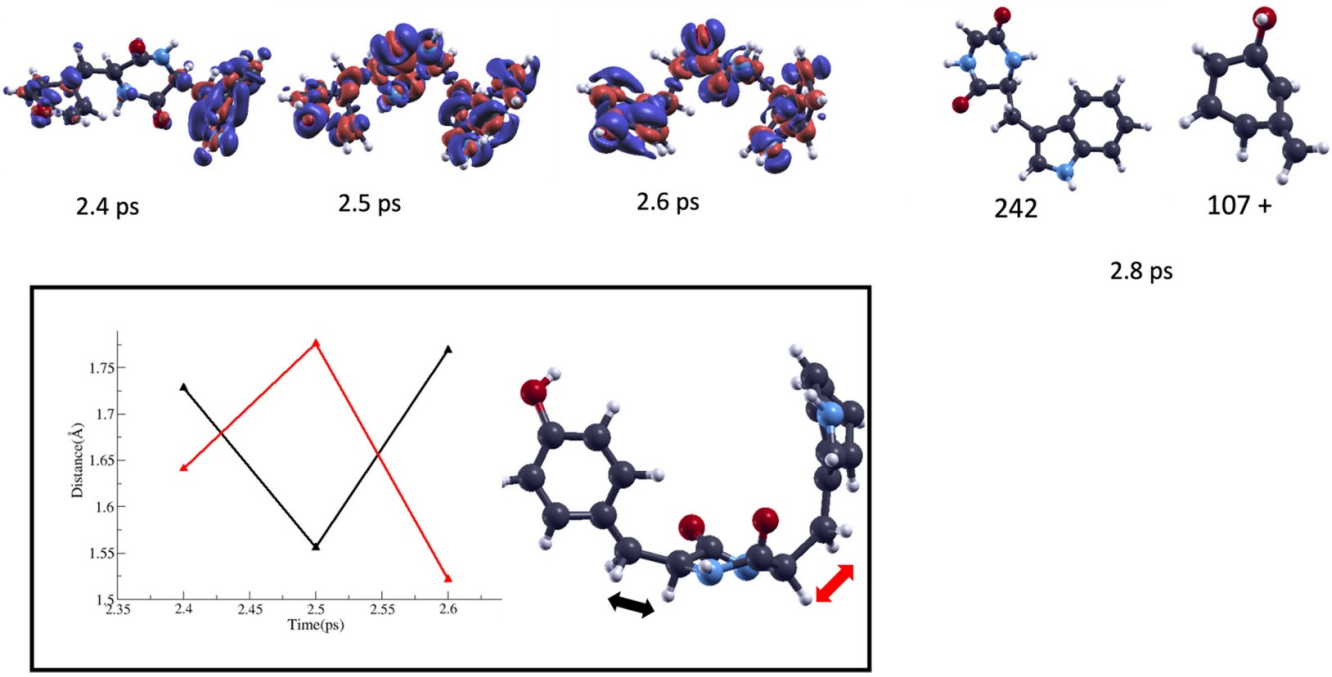

Figure 9. Top panel: charge difference calculated at B3LYP level of theory between neutral and cationic state of c-TrpTyr in selected QCxMS MD snapshots, representing a fragmentation pathway leading from 349^{+} to 242 and 107^{+}. Bottom panel: CH_2–CH distance between DKP and phenol ring (black line) and DKP and indole ring (red line) as a function of time, with the schematic of the molecular structure on the right side.

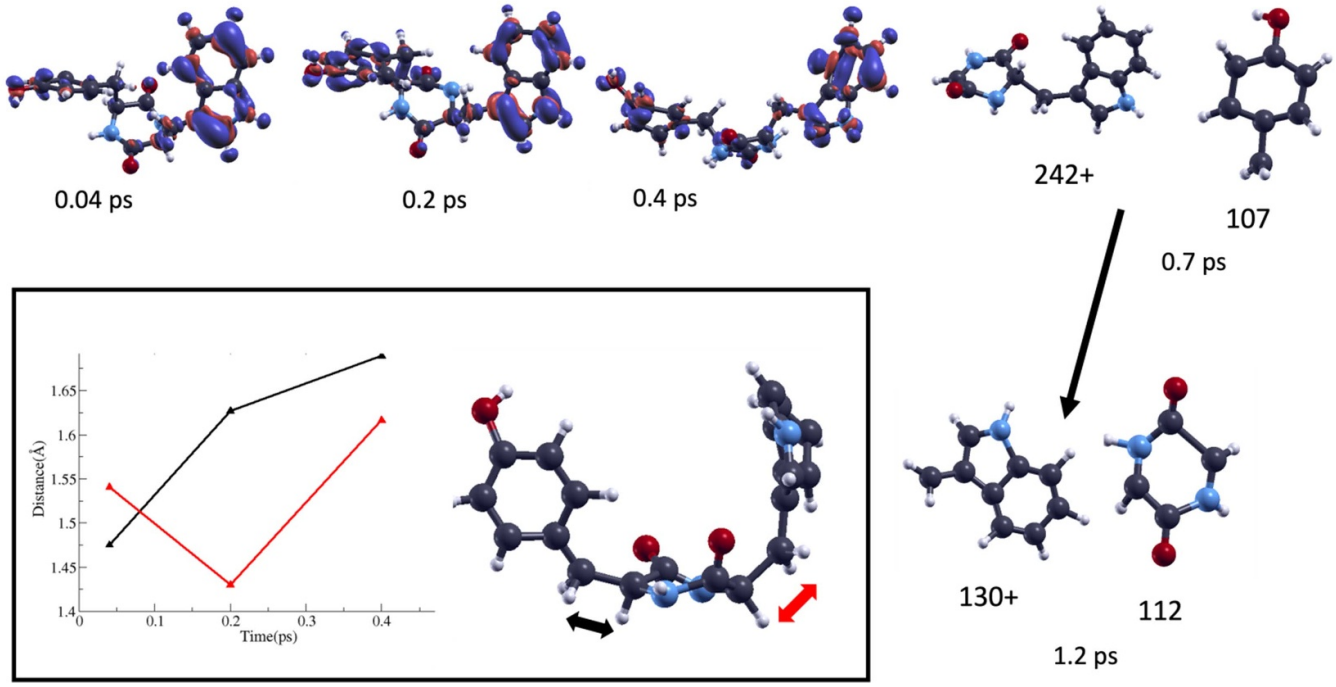

Figure 10. Top panel: charge difference calculated at B3LYP level of theory between neutral and cationic state of c-TrpTyr in selected QCxMS MD snapshots, representing a fragmentation pathway leading to the production of 242^{+} and its further fragmentation in 130^{+} and 112. Box in the bottom panel: CH_2-CH distance between DKP and phenol ring (black line) and DKP and indole ring (red line) as a function of time, with the schematic of the molecular structure on the right side.

(see also figure S8). The analysis suggests again a coupling between charge localization and vibrational behavior of the involved CH_2–CH bond, leading to the rapid fragmentation of 242^{+} with the release of the 130^{+} and 112 fragments. This result can explain the observation in the PEPICO measurements of a very low intensity of the fragment 242^{+} with respect to

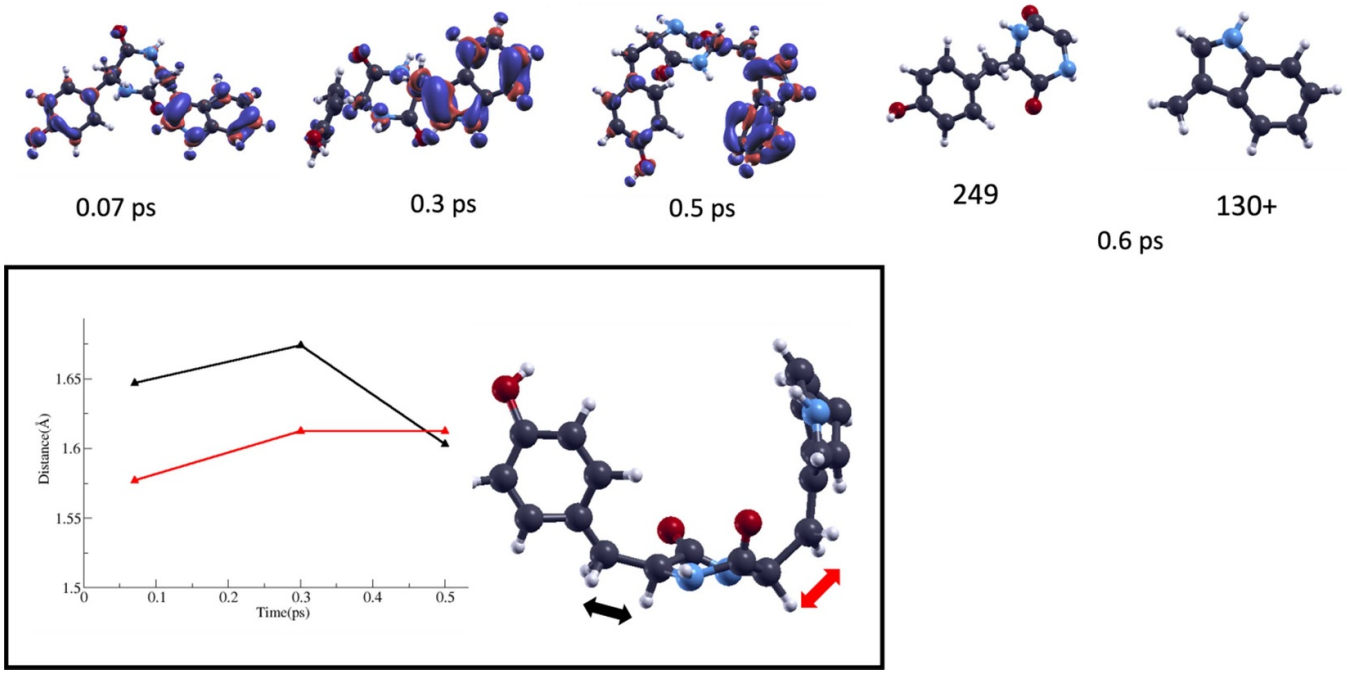

Figure 11. Top panel: charge difference calculated at B3LYP level of theory between neutral and cationic state of c-TrpTyr in selected QCxMS MD snapshots, representing a fragmentation pathway leading to the production of 130^+ and 249 (right side). Bottom panel: CH_2–CH distance between DKP and phenol ring (black line) and DKP and indole ring (red line) as a function of time, with the schematic of the molecular structure on the right side.

130^+ fragment (figure 5), despite their close formation energies reported in the analysis of the potential energy surfaces (figure 7).

Finally, figure 11 shows the highly favored direct formation of the 130^+ fragment from the parent ion, with a notable localization of charge depletion on the indole group, evident in the selected snapshot preceding the dissociation. Detachment of 130^+ is favored by a concurrent elongation of the CH_2–CH on the phenol side, which hinder the transfer of positive charge on the other side of the molecule. A statistical analysis of MD trajectories suggests that the higher abundance of 130^+ can be attributed to the direct dissociation of the charged indole from the parent ion. The production of 130^+ in both c-TrpTrp and c-TrpTyr (as highlighted in figure S9) from the fragmentation of 243^+ amounts to less than 0.3%–0.2%, while the one from the fragmentation of 242^+ amounts to about 3%–4%.

6. Conclusions

The fragmentation following photoionization of three cyclic dipeptides with at least one aromatic amino acid has been studied by PEPICO measurements. The possible fragmentation pathways have been also characterized by the theoretical exploration of the potential energy surfaces and by the analysis of charge localization and of high internal energy molecular dynamics trajectories. The results of this joint experimental-theoretical study agree in the indication of (i) a large dominance of the production of a charged fragment including the indole chromophore independently of the energy transferred to the neutral target and the ionized orbital in both c-TrpTrp and c-TrpTyr and (ii) a prevalence for the production of a fragment containing the phenyl chromophore in the case of c-GlyPhe.

PEPICO experiments with synchrotron radiation are unable to distinguish between charge transfer and charge migration, however it is plausible to interpret the experimental observations together with the calculated difference of the electronic density distribution between the neutral molecules and cations, as due to a fast internal conversion after photoionization to the HOMO of the cation followed by a statistical redistribution of the excess energy among the different vibrational degree of freedom, which in turn lead to fragmentation. These findings are further supported by the analysis of charge distribution along selected fragmentation trajectories based on molecular dynamics simulations. Theoretical results reveal that a predominant charge localization on specific aromatic substituents, resulting in their high abundance in the mass spectra almost irrespective of incident photon energy, is closely coupled to the vibrational motion of the -CH_2–CH linkers connecting aromatic side chains with the DKP backbone, which drives the fragmentation of the molecules. The results can be rationalized considering the relative energy gap between the ionization energy of orbitals localized on the aromatic chromophore and the DKP ring and the mixing between these orbitals. In a local picture, the molecular ion tries to optimize its energy by ‘intramolecular hopping’ [39–42] of the hole to the chromophore which has the lowest IP. This mechanism, named by Chattoraj *et al* [19] ‘natural electron(hole)-transfer’, can occur in molecular ions directly after ionization, in a time scale shorter than 2 ns in the presence of an aromatic terminal such as benzene, indole, and

biphenyl, with no intrinsic restriction for distance of the charge transfer [51].

According to the work of Weinkauf *et al* on the electron mobility and dissociation in linear peptides by resonant ionization mass spectrometry [6], in presence of the Trp amino acid there is a strong stabilization of the positive charge on the indole ring which determines the selectivity of the fragmentation process. This is consistent with the finding of the present work, also in cyclo-dipeptide. However, the presence of other amino acids in linear peptides may create a barrier for the charge transfer mechanism, as observed in the case of linear tripeptides containing Trp terminal amino acid [7]. On the contrary, it is shown here that the presence of a central DKP ring in cyclo-dipeptides does not hamper the charge transfer, allowing the hole hopping between two aromatic side chains directly after ionization, as clearly observed in the case of c-TrpTyr.

Data availability statement

All data that support the findings of this study are included within the article (and any supplementary files).

Acknowledgments

The present work was performed in the framework of the PRIN20173B72NB research project 'Predicting and controlling the fate of biomolecules driven by extreme-ultraviolet radiation', the COST action CA18212—Molecular Dynamics in the GAS phase (MD-GAS) supported by COST (European Cooperation in Science and Technology) and the European Research Council (ERC) under the European Union's Horizon 2020 research and innovation program (Grant Agreement No. 951224, TOMATTO).

ORCID iDs

Laura Carlini https://orcid.org/0000-0001-9448-017X
Paola Bolognesi https://orcid.org/0000-0002-6543-6628
Federico Vismarra https://orcid.org/0000-0002-2348-2749
Mauro Nisoli https://orcid.org/0000-0003-2309-732X
Mohammadhassan Valadan https://orcid.org/0000-0001-8656-9510
Lorenzo Avaldi https://orcid.org/0000-0002-2990-7330

References

[1] Danger G, Plasson R and Pascal R 2012 *Chem. Soc. Rev.* **41** 5416
[2] Schlag E W, Yang D-Y, Sheu S-Y, Selzle H L, Lin S H and Rentzepis P M 2000 *Proc. Natl Acad. Sci.* **97** 9849
[3] Yan X, Zhu P and Li J 2010 *Chem. Soc. Rev.* **39** 1877
[4] Ziganshin M A, Safiullina A S, Zingashina S A, Gerasimov A V and Gorbatchuk V V 2017 *Phys. Chem. Chem. Phys.* **19** 13788–97
[5] Govindaraju T, Pandeeswar M, Jayaramulu K, Jaipuria G and Atreya H S 2011 *Supramol. Chem.* **23** 487
[6] Weinkauf R, Schanen P, Yang D, Soukara S and Schlag E W 1995 *J. Phys. Chem.* **99** 11255
[7] Weinkauf R, Schanen P, Metsala A, Schlag E W, Bürgle M and Kessler H 1996 *J. Phys. Chem.* **100** 18567
[8] Remacle F and Levine R D 2007 *Z. Phys. Chem.* **221** 647–61
[9] Remacle F and Levine R D 2006 *Proc. Natl Acad. Sci.* **103** 6793–8
[10] Remacle F, Levine R D and Ratner M A 1998 *Chem. Phys. Lett.* **285** 25–33
[11] Cederbaum L and Zobeley J 1999 *Chem. Phys. Lett.* **307** 205
[12] Worner H J *et al* 2017 *Struct. Dyn.* **4** 061508
[13] Calegari F *et al* 2014 *Science* **346** 336
[14] Cryan J P, Driver T, Duris J, Guo Z, Li S, O'Neal J T and Marinelli A 2022 *Adv. At. Mol. Opt. Phys.* **71** 1–64
[15] Ahn T K, Avenson T J, Ballottari M, Cheng Y-C, Niyogi K K, Bassi R and Fleming G R 2008 *Science* **320** 794
[16] Artes J M, Lopez-Martinez M, Diez-Perez I, Sanz F and Gorostiza P 2014 *Electrochim. Acta* **140** 83
[17] Giese B, Graber M and Cordes M 2008 *Curr. Opin. Chem. Biol.* **12** 755
[18] Stevenson D P 1951 *Disc. Faraday Soc.* **10** 35
[19] Chattoraj M, Laursen S L, Paulson B, Chung D D, Closs G L and Levy D H 1992 *J. Phys. Chem.* **96** 8778
[20] Derossi A, Lama F, Piacentini M, Prosperi T and Zema N 1995 *Rev. Sci. Instrum.* **66** 1718
[21] Plekan O, Coreno M, Feyer V, Moise A, Richter R, De Simone M, Sankari R and Prince K C 2008 *Phys. Scr.* **78** 058105
[22] Cautero G, Sergo R, Stebel L, Lacovig P, Pittana P, Predonzani M and Carrato S 2008 *Nucl. Instrum. Methods Phys. Res.* A **595** 447
[23] Menk R H *et al* 2019 *AIP Conf. Proc.* **2054** 067001
[24] Carlini L *et al* 2023 *J. Chem. Phys.* **158** 054201
[25] Carlini L, Chiarinelli L, Mattioli G, Castrovilli M C, Valentini V, De Stefani A, Bauer E M, Bolognesi P and Avaldi L 2022 *J. Phys. Chem.* B **126** 2968–78
[26] Cartoni A, Bolognesi P, Fainelli E and Avaldi L 2014 *J. Chem. Phys.* **140** 184307
[27] Raghavachari K, Trucks G W, Pople J A and Head-Gordon M A 1989 *Chem. Phys. Lett.* **157** 479–83
[28] Frisch M J, Trucks G W, Schlegel H B, Scuseria G E, Robb M A, Cheeseman J R, Scalmani G, Barone V, Mennucci B and Petersson G A 2009 *Gaussian 09, Revision A. 02* (Gaussian, Inc.)
[29] Wong M W 1996 *Chem. Phys. Lett.* **256** 391–9
[30] Gonzalez C and Schlegel H B 1989 *J. Chem. Phys.* **90** 2154
[31] Gonzalez C and Schlegel H B 1990 *J. Phys. Chem.* **94** 5523
[32] Molteni E *et al* 2021 *Phys. Chem. Chem. Phys.* **23** 26793
[33] Giannozzi P *et al* 2017 *J. Phys.: Condens. Matter* **29** 465901
[34] Giannozzi P *et al* 2009 *J. Phys.: Condens. Matter* **21** 395502
[35] Grimme S 2013 *Angew. Chem., Int. Ed.* **52** 6306–12
[36] Asgeirsson V, Bauer C and Grimme S 2017 *Chem. Sci.* **8** 4879
[37] Seki K and Inokuchi H 1979 *Chem. Phys. Lett.* **65** 158
[38] Campbell S, Beauchamp J L, Rempe M and Lichtenberger D L 1992 *Int. J. Mass Spectrom. Ion Process.* **117** 83
[39] WilsonK R, Jimenez-Cruz M, Nicolas C, Belau L, Leone S R and Ahmed M 2006 *J. Phys. Chem.* A **110** 2106
[40] Campbell S, Marzluff E M, Rodgers M T, Beauchamp J L, Rempe M E, Schwinck K F and Lichtenbergert D L 1994 *J. Am. Chem. Soc.* **116** 5257
[41] Plekan O, Feyer V, Richter R, Coreno M and Prince K C 2008 *Mol. Phys.* **106** 1143
[42] Yu D, Rauk A and Armstrong D A 1995 *J. Am. Chem. Soc.* **117** 1789
[43] Chiarinelli J, Bolognesi P, Domaracka A, Rousseau P, Castrovilli M C, Richter R, Chatterjee S, Wang F and Avaldi L 2018 *Phys. Chem. Chem. Phys.* **20** 22841
[44] Arachchilage A P W, Wang F, Feyer V, Plekan O and Prince K C 2010 *J. Chem. Phys.* **133** 174319

[45] Arachchilage A P W, Wang F, Feyer V, Plekan O and Prince K C 2012 *J. Chem. Phys.* **136** 124301
[46] Gross D and Grodsky G 1955 *J. Am. Chem. Soc.* **77** 1678
[47] Guo Y, Cao S, Zong X, Liao X and Zhao Y 2009 *Spectroscopy* **23** 131
[48] Guo Y, Cao S, Wei D, Zong X, Yuan X, Tang M and Zhao Y 2009 *J. Mass Spectrom.* **44** 1188
[49] Rice O K and Ramsperger H C 1927 *J. Am. Chem. Soc.* **49** 1617
[50] Aguirre N F, Dıaz-Tendero S, Hervieux P-A, Alcamì M and Martin F 2017 *J. Chem. Theory Comput.* **13** 992
[51] Jortner J, Bixon M, Heitele H and Michel-Beyerle M E 1992 *Chem. Phys. Lett.* **197** 131